



CFD Based Numerical Analysis of Flow-Field Characteristics on Airfoils Experiencing Transverse Flow

C. Seidel¹, R.LeBeau², S. Jayaram^{3*}

¹Department of Mechanical Engineering and Materials Science, Washington University in Saint Louis, St. Louis, USA

^{2,3}Department of Aerospace and Mechanical Engineering, Saint Louis University, St. Louis, USA

*Corresponding Author: sanjay.jayaram@slu.edu, Tel.: 314-977-8212

DOI: <https://doi.org/10.26438/ijcse/v7i2.463468> | Available online at: www.ijcseonline.org

Accepted: 15/Feb/2018, Published: 28/Feb/2019

Abstract— In the presented work, the flow-field around dropped airfoils was investigated to establish a correlation with transverse flow on a flat plate. This scenario relates to falling maple seeds and developing a fundamental understanding of the how the forces and drag coefficients develop prior to rotation. Understanding the development of these forces will lead to understanding the characteristics of maple seeds (and other auto-rotating seeds) that cause auto-rotation and development of leading-edge vortices. Using CFD, a thin, almost 2D airfoil was placed in a 3D environment and dropped through free space. Flow around the dropped airfoil was accelerated by gravity considerations. The resulting surface forces were evaluated through comparison of coefficient of drag values for transverse flow on a flat plate. The analysis of the forces demonstrated that the drag coefficient values on the lower surface of NACA 0012 and E63 airfoils profile were found to be similar to the flat plate values. The convex NACA 0012 airfoil experienced larger surface forces than flat plate and the concave E63 airfoil experienced smaller surface forces than flat plate. This work also demonstrates that coefficient of drag varies with time.

Keywords—Transverse Flow, Cross-flow, NACA 0012, Dropped Airfoil, Flat Plate, Perpendicular Flow

I. INTRODUCTION

The biomimetic inspiration of samara seeds for single rotor unmanned aerial vehicles [1][2] and wind turbine blades [3][4] has created an increased interest in understanding the underlying flow field physics of samara seeds. One of the focal points of current studies is the generation of leading edge vortices (LEVs) and its impact on the increased lift-to-drag ratio [5][6]. These same studies have illustrated flow-field properties of dynamic systems and horizontal flow systems to demonstrate the formation of LEVs [5][6]. Other works model the dynamic equations of the forces within the system [7][8], including the resultant lift on the lower surface of the wing caused by the vertical fluid force due to descent.

A noticeable gap exists in literature on the characteristics of flow fields around airfoils generated by a freestream flow transverse to the chord, both experimentally and theoretically. Current work that studies flow that is transverse to the planform surface of the wing or blade sections is in the areas of wind turbines [9] and samara seeds [5-8]. However, many of these studies are on the mechanics and dynamics of the system and not the surrounding fluid field. Wind turbine and samara seed studies also investigate transverse flows in a rotating system [7][9]. An understanding of the flow field transverse to the planform surfaces of wings in a rotationally

static system is not as developed, particularly for accelerating flows like those encountered by falling seeds. This inspired a deeper investigation into flow characteristics for symmetric (NACA 0012) and asymmetric (Eppler 63, E63) airfoil. This work explores the development of the fluid field analysis of the drag coefficient (C_D) of NACA 0012 and E63 airfoils for the purpose of validating the C_D values with the C_D of a flat plate in transverse flow.

The rest of the paper is organized as follows: Section II discusses related work; Section III discusses the methodologies utilized, including experimental approach, software and simulation environment, and design and optimization of mesh; Section IV discusses the experimental results; and Section V provides a future scope and concludes the paper.

II. RELATED WORK

In gaining an understanding of the development of drag forces on a dropped airfoil, a more solid foundation of the fundamentals of flight dynamics for samara seeds can be obtained. CFD simulations of samara seeds have been studied, but the cause of the generation of LEVs has not entirely been quantified [3]. Investigating drag generated through descent provides the first step to developing this fundamental understanding. This section details related work

in high angle of attack and transverse flow for airfoils, blades, and flat plates.

Sørensen and Michelsen [10] used CFD to investigate the drag for blades at high angle of attack and compared with a flat plate for transverse flow. The time step size and mesh were varied for infinite flat plate simulations. There was a significant variation for the calculated C_D with respect to time, but only a minor variation with respect to different mesh. When changing to a finite flat plate with varied aspect ratios (2, 20, and 40) and the simulations proved to be similar to the measured data for C_D . For the blades, Sørensen and Michelsen only investigated the case of 90°.

Tian et al. investigated flow normal to a circular disk through large-eddy simulation (LES) [11]. The simulated C_D values were close to the finite flat plate values of Sørensen and Michelsen [10]. The work focused primarily on the vortices generated in the wake and wake instability.

Parked conditions for wind turbines have been investigated by several researchers including Ostawari and Naik [12], Cox and Echtermeyer [13], Dahlberg et al. [14], and Shirzadeh et al. [15]. Ostawari and Naik focused specifically on untwisted blades with cross-sections in the NACA 44xx family [12]. Cox and Echtermeyer primarily focused on the structural integrity and design of a blade with twist in extreme loading conditions [13]. The results centered around the twist of the blade and tip deflection. Dahlberg et al. studied a small wind turbine in a wind tunnel with parked conditions [14]. Shirzadeh et al. compared simulated and measured data for offshore wind turbines in parked conditions, but primarily focused the work on frequency and damping data [15].

Pesavento and Wang studied the motion of a free-falling body (plate) using two dimensional Navier-Stokes equations [16]. The investigation revealed that the forces on the plate are dominated by a product of the linear and angular velocity terms. This is in contrast to an airfoil which is dominated by velocity squared for lifting forces. The work also introduces an instantaneous circulation, which is viewed as missing from traditional lift methods.

To the best of our knowledge, there is no known literature that addresses transverse flow or dropped airfoils, specifically in a nearly 2D case, for the purpose of understanding the development of drag forces on the surface. The same can be said for flat plate simulations. Wind turbines with parked loads is a more present area of related research but is not gravity driven and many of the blades contain twist from root to tip. A constant angle of attack that varies only slightly from the transverse nature is a consideration for the study. In addition, the focus of this work is to begin investigations on dropped airfoils where the

airfoil geometry is a key consideration, which is not an active consideration in much of the related work.

III. APPROACH AND METHODOLOGY

A collection of investigations on wind turbines and samara seeds exist for dynamics of systems, flow-field trends in rotating systems, and LEV formation in horizontal flow over a static maple seed. None of these investigations single out the flow-field trends related to the forces perpendicular to the surface of the blade. In a samara seed, the flow caused by the descent of the seed creates a drag force on the lower surface of the wing. Some horizontal axis wind turbine blades experience a similar load from the transverse flows that power them. This work investigates the flow-fields and surface forces for NACA 0012 and E63 airfoils to understand the differences between a symmetric and an asymmetric airfoil.

A. Experimental Approach

A flat plate was selected for comparison because the ratio of chord length to thickness of the airfoil section resembles that of a flat plate. Another consideration was the rounded nature of the leading edge of the airfoil, but with sharp trailing edge. It was hypothesized that the leading edge would result in a smooth transition of flow around the airfoil, while the trailing edge would behave in a manner similar to the sharp edges of a flat plate, but differing in thickness. The final area of focus was to observe the impact of the curvature of an airfoil on the drag of the system. In particular, focusing on how an airfoil with a concave lower (E63) behaves differently than an airfoil with a convex lower surface (NACA 0012).

The transverse flow characteristics of an airfoil are anticipated to be similar to that of a flat plate (Figure 1). The actual profiles for the airfoils are expected to vary to some degree due to geometric difference between the flat plate and airfoil, especially at the leading and trailing edges. For transverse flow on a flat plate, the forces transverse to the surface are often denoted as drag. The standard drag coefficient (C_D) value for flat plates in turbulent flow varies between sources, partially due to the geometry of the flat plate. Simiu and Scanlan [17] provide the most complete representation C_D with a range of ~0.8-2.8 that is dependent on the ratio of length to height of the plate. Hoerner [18] states that a 2D flat plate has a C_D of 1.98 and the C_D of a 3D flat plate is 1.17. Nedic [19] agrees with Hoerner [18] with a C_D of 1.17. Proceedings for the Low Reynolds Number Aerodynamics Conference [20] provides a slightly larger C_D of 1.28. For this work, we compare to drag forces to these values of C_D plus 2.1 as an upper limit, which is within the range proposed by Simiu and Scanlan [17]. In this paper, the force transverse to the planform will be referred to as drag forces to remain consistent with the C_D origins.

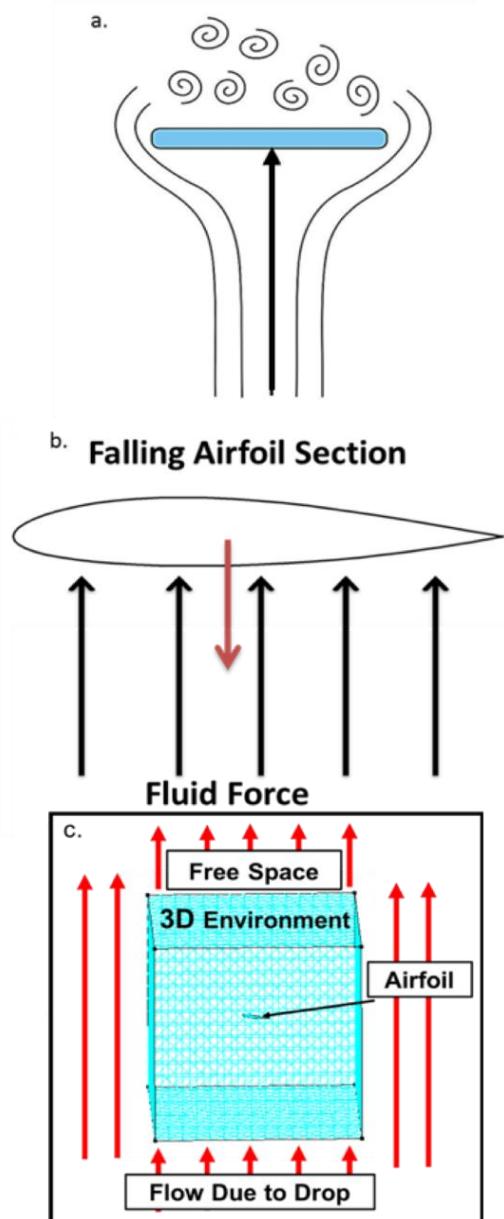


Figure 1: Flow expectations for: a) transverse flow on a flat plate b) transverse flow on an airfoil section c) environment of drop simulation tests where flows in through the bottom and out through the top

B. Software and Methods

CFD simulations were conducted in SC/Tetra. The airfoil drop simulations comprised of free space, a 3D environment, and a thin, pseudo 2D airfoil, (Figure 1c). While simulating in a 2D environment is less computationally expensive, the desire to allow a full blade to rotate in future analysis made the 3D environment approach more compelling even when the airfoil grid was effectively 2D. The entire environment dropped through free space at gravitational acceleration, starting from rest. The gravitational acceleration did not take into account drag effects that would alter the velocity, i.e. $v = gt$. Transient analysis was selected as the solution process to

control the length of real time over which the airfoil falls. The boundary parameters were set to allow the inflow on the bottom surface in the system to accelerate at a gravitational rate and the flow out of the system was not restricted. The full vertical domain was 10 chord lengths with the airfoil centrally located. The free-slip side boundaries were set at five chord lengths from the leading and trailing edge to limit blocking effects and ensure that the field could fully develop. The system was dropped for two real time seconds with data recorded every 0.01 seconds. The system remains laminar throughout the entire process as the maximum Reynolds number reached is 1.33×10^4 , based on chord length.

Using the described method, two sets of degrees of freedom were required. The degrees of freedom are relative to the coordinate axes in for the samara seed shown in Figure 2. The first set of degrees of freedom was for the airfoil within the 3D environment and the second was for the 3D environment in the free space. The airfoil was fixed in location relative to the 3D environment, but the 3D environment was allowed to translate in all directions relative to the free space to simulate falling. Therefore, any translation of the airfoil is relative to the free space and not the 3D environment. The rotational directions of the airfoil and 3D environment were fixed for these simulations because they are not self-balancing like samara seeds. The purpose of this work was to obtain transverse flow data for predictive methods with the intention to expand imparting rotation in future work.

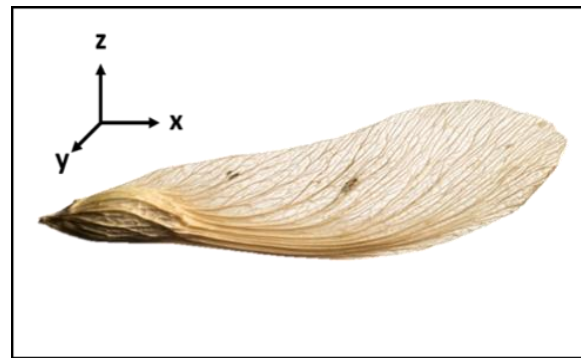


Figure 2: Coordinate system in relation to samara seed orientation

C. Mesh Characteristics and Optimization

The meshes used around the airfoil consist of a relatively thin structured grid with the rest of the domain filled with an unstructured mesh. Design of the unstructured portion is approximately defined by regions of relative mesh density and total mesh size, but grid details will vary beyond user control. The structured, or prism mesh, is more precisely defined by the number of points about the airfoil surface, the initial normal spacing of the surface layer, the number of layers extending from the surface, and the rate of stretching

of the layer thickness from the initial, defined layer. Meshes were assessed on their Courant-Friedrichs-Lowy (CFL) condition and maximum non-dimensional wall distance (y^+) value. The CFL condition measures the iterative stability of the time dependent partial differential equations. The y^+ value demonstrates how coarse or fine the mesh is at the surface of the airfoil. The wall distance is defined as

$$y^+ = \frac{u_* y}{v}, \quad (1)$$

where y is the thickness of the initial layer, u_* is the friction velocity defined as the square root of the shear stress at the surface divided by density, and v is the kinematic viscosity. The CFL criterion is

$$C = \Delta t \sum_{i=1}^n \frac{u_{x_i}}{\Delta x_i} \leq C_{max} \quad (2)$$

where C represents the CFL condition number, Δt is the time step, u_{x_i} is the magnitude of velocity, Δx_i is the smallest element size, and n is the number of dimensions the CFL is calculated in. For a given timestep, a small element size yields a small y^+ value but increases the CFL number. The CFL number can then be reduced by reducing the timestep, but that can unacceptably increase the runtime.

In order to optimize the simulation run time, a fixed timestep of 0.0001 seconds (10,000 steps per second) was used. This timestep was used to simulate the performance of 8 mesh constructions for the NACA 0012 at 7° AoA. The number of elements in the mesh ranged from 800,000 to 1.5 million, with initial layer thicknesses of 0.078 to 0.2 mm, 25-27 prism layers, and stretching value range of 1.1-1.3. Meshes were assessed based on trying to minimize the y^+ and CFL values while not generating excessive computation time. The selected mesh had 908K elements with a maximum y^+ of 12.25 and an average C of 0.71 after 5 seconds. The maximum local CFL value at 5 seconds did exceed the desired limit of $C_{max} = 1$ on many elements, but at the targeted simulation limit of two seconds (20,000 steps) all element CFL values were below one.

IV. RESULTS AND DISCUSSION

The NACA 0012 and E63 airfoils were simulated for angles of attack of 0° , 2° , 5° , and 7° . The 0° AoA case for each airfoil was viewed as a baseline for comparison to flat plate coefficients, defined here as when the airfoil chord is perpendicular to the fall direction. The full comparison of the drag force over time between all angles of attack for the

NACA 0012 and E63 airfoils are presented graphically in Figure 3a. Due to the similarity in results across the AoAs, only the 7° AoA for each airfoil is compared to the flat plates is represented in Figure 3b. The 7° AoA was selected because it is close to a theoretical AoA for a maple seed. The C_D values for the drag forces on flat plates were assumed to be constant over time. While both airfoils projected near the C_D values of 1.17 and 1.28, the NACA 0012 profiled above and the E63 below. This suggests that a convex lower surface exhibits a drag force greater than that of the flat plate approximation and a concave surface for a transverse flow case.

A final observation to note from Figure 3b is that the profile of the drag force on the lower surface becomes more linear with time, thus depicting an underlying variation in the drag calculation. The drag force on the airfoils in Figure 3b appear to become more linear with time, depicting a time variation of the C_D , which is validated in Figure 4. The change of rate of the C_D in each system is attributed to the pressure field stabilizing as the flow develops and could fully stabilize when the flow around the airfoil is fully developed.

V. CONCLUSION AND FUTURE SCOPE

The presented study of transverse flows on airfoil sections provides initial understanding of the flow physics and demonstrates the importance of the curvature of the airfoil on generation of forces caused by transverse flow. The convex NACA 0012 resulted in a drag force of approximately 3.30 N for all tested angles of attack after falling for two seconds. Meanwhile, the concave E63 airfoil had a smaller drag force of 2.3 N for all tested angles of attack after two seconds. The drag forces on the airfoil continue to adjust with time, making the direct comparison to the flat plate drag forces and C_D less precise due to the use of a constant C_D . Numerically, the NACA 0012 airfoil drag force at two seconds is larger than that of the flat plates with C_D values of 1.28 and 1.17 and continues to diverge, indicating that a longer simulated time would result in an increasing difference between the flat plates and the NACA 0012 airfoil. Conversely, the E63 airfoil drag coefficient was initially higher than the two flat plate cases but continued to decrease until it was less than the flat plate standard at the two second mark. The rate of variation is due to a dynamic C_D value. Further studies on the effects of edge geometry and lower surface concavity would be beneficial to determine the cause of the diverging trends. Despite the lack of C_D variance with time for the flat plates, the results demonstrated that a flat plate can be a reasonable comparison for estimation of transverse flow on an airfoil.

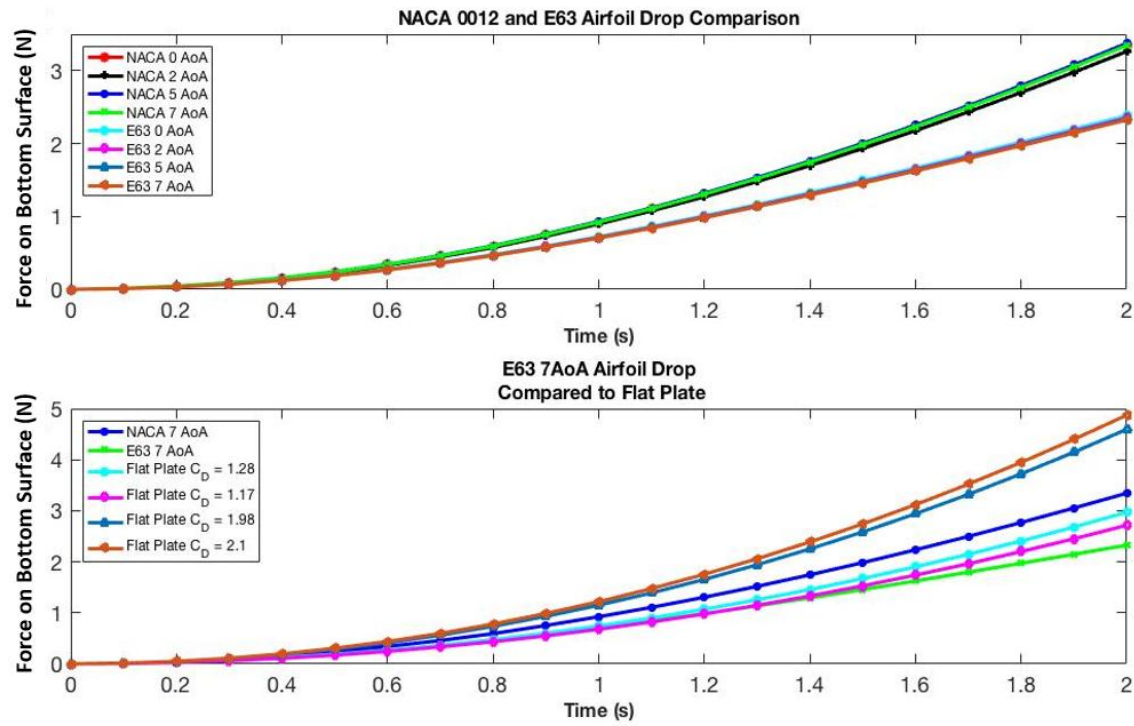


Figure 3: a) NACA 0012 and E63 airfoil drop drag force on lower surface comparison for all angles of attack, b) Force on lower surface of dropped NACA 0012 and E63 airfoils at 7° compared to calculated forces on lower surface of flat plates with varying C_D

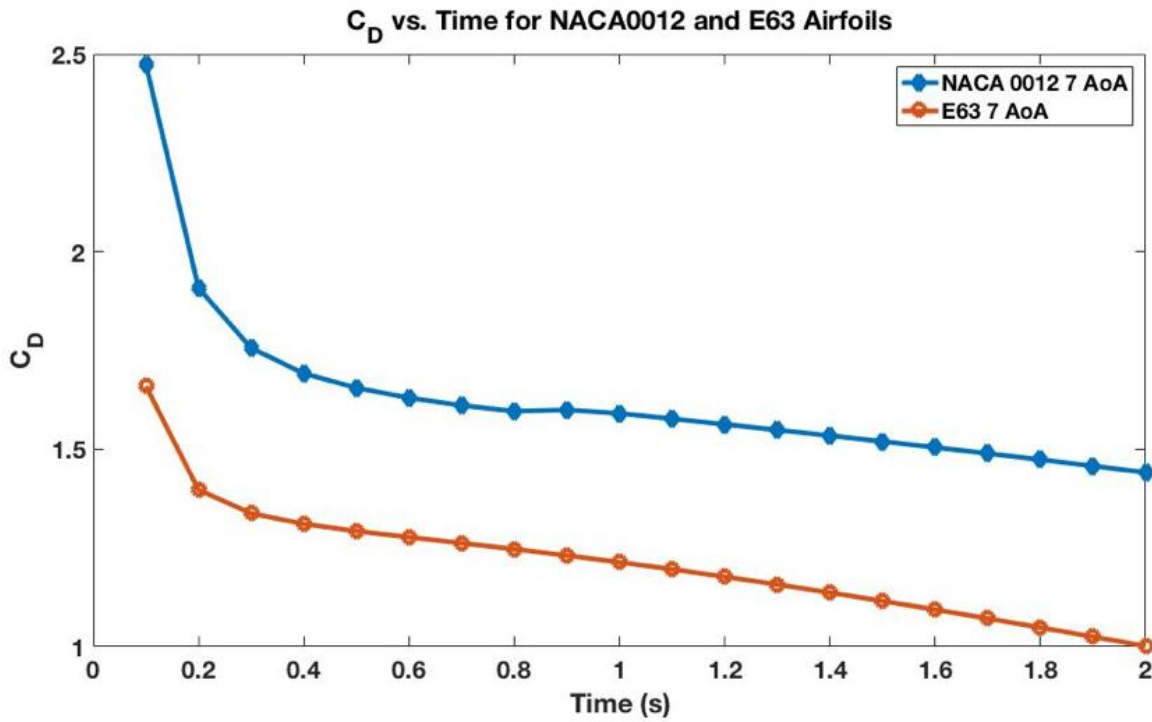


Figure 4: Variation in C_D over time for NACA 0012 and E63 airfoils at 7° AoA

REFERENCES

[1] K. Fregene, D. Sharp, C. Bolden, J. King, C. Stoneking, S. Jameson, "Autonomous Guidance and Control of a Biomimetic Single-Wing MAV", In the Proceedings of the Unmanned Systems Conference; pp. 1-12, 2016.

[2] S. Jameson, B. Satterfield, C. Bolden, N. Allen, H. Youngren, "SAMARAI nano air vehicle a revolution in flight", In the proceedings of Association for Unmanned Vehicle Systems International Unmanned Systems North America; pp. 1-15, 2007.

[3] J. R. Holden, T. M. Caley, and M. G. Turner, "Maple Seed Performance as a Wind Turbine," In the Proceedings of 53rd AIAA Aerospace Sciences Meeting, 2015.

[4] R. K. V. Gadamsetty, J. Loganathan, V. K. Balaramudu, and A. Rao, "Alternate Wind Turbine Blade Planform Design Studies for Low Wind Speeds," Volume 9: Oil and Gas Applications; Supercritical CO₂ Power Cycles; Wind Energy, 2015.

[5] D. Lentink, W. B. Dickson, J. L. V. Leeuwen, and M. H. Dickinson, "Leading-Edge Vortices Elevate Lift of Autorotating Plant Seeds," *Science*, vol. 324, no. 5933, pp. 1438-1440, 2009.

[6] I.H. Arroyo, D. Rezgui, R. Theunissen, "Analytical Model for Leading-Edge Vortex Lift on Rotating Samara Seeds: Development and Validation," In Proceedings of Applied Aerodynamics Conference 2016, United Kingdom, 2016.

[7] C.L. Ladera, and P. A. Pineda. "The Physics of the Spectacular Flight of the Triplaris Samaras." *Latin-American Journal of Physics Education* vol. 3, no. 3, pp. 557-565, 2009.

[8] R. Fang, Y. Zhang, and Y. Liu, "Aerodynamics and Flight Dynamics of Free-Falling Ash Seeds," *World Journal of Engineering and Technology*, vol. 5, no. 4, pp. 105-116, 2017.

[9] W. Hu, K. K. Choi, O. Zhupanska, and J. H. Buchholz, "Integrating variable wind load, aerodynamic, and structural analyses towards accurate fatigue life prediction in composite wind turbine blades," *Structural and Multidisciplinary Optimization*, vol. 53, no. 3, pp. 375-394, 2015.

[10] N. Sørensen and J. Michelsen, "Drag Prediction for Blades at High Angle of Attack Using CFD," 42nd AIAA Aerospace Sciences Meeting and Exhibit, 2004.

[11] X. Tian, M. C. Ong, J. Yang, and D. Myrhaug, "Large-eddy simulations of flow normal to a circular disk at Re=1.5×10⁵," *Computers & Fluids*, vol. 140, pp. 422-434, 2016.

[12] C. Ostowari and D. Naik, "Post-stall wind tunnel data for NACA 44XX series airfoil sections," *Wind Engineering*, vol. 8, no. 3, pp. 176-194, 1985.

[13] K. Cox and A. Echtermeyer, "Structural Design and Analysis of a 10MW Wind Turbine Blade," *Energy Procedia*, vol. 24, pp. 194-201, 2012.

[14] J.A. Dahlberg, G. Ronsten, "A Wind Tunnel Investigation of Tower Blockage Effects and Parking Loads on a E 5.35 M Horizontal Axis Wind Turbine," In 5th European Wind Energy Association Conference and Exhibition; pp. 414-417, 1994.

[15] R. Shirzadeh, W. Weijtjens, P. Guillaume, and C. Devriendt, "The dynamics of an offshore wind turbine in parked conditions: a comparison between simulations and measurements," *Wind Energy*, vol. 18, no. 10, pp. 1685-1702, 2014.

[16] K. Cox and A. Echtermeyer, "Structural Design and Analysis of a 10MW Wind Turbine Blade," *Energy Procedia*, vol. 24, pp. 194-201, 2012.

[17] E. Simiu, and R.H. Scanlan, "Wind effects on structures: Fundamentals and application to design." John Wiley & Sons Inc Publisher, USA 1996.

[18] S. F. Hoerner, *Fluid-dynamic drag*. Brick Town, NJ: Hoerner Fluid Dynamics, 1965.

[19] J. Nedić, B. Ganapathisubramani, and J. C. Vassilicos, "Drag and near wake characteristics of flat plates normal to the flow with fractal edge geometries," *Fluid Dynamics Research*, vol. 45, no. 6, 2013.

[20] T. J. Mueller, *Low Reynolds number aerodynamics: proceedings of the conference, Notre Dame, Indiana, USA, 5-7 June 1989*. New York: Springer-Verlag, 1989.

Authors Profile

Cory Seidel received a Bachelor of Science in Mechanical Engineering in 2015 from and Master of Science in 2016 from Saint Louis University. He is currently pursuing his PhD at Washington University in St. Louis. Cory is a member of Tau Beta Pi, the Vertical Flight Society, and AIAA. His research interests include computational fluid dynamics, wind energy, urban renewable energy, and machine learning. Outside of academic studies, Cory has spent four summers as a research intern at Wright-Patterson Air Force Base. His work focused on uncertainty quantification in fabrication processes and artificial target generation and data analysis using machine learning algorithms.



R.P. LeBeau, Jr., Ph.D., P.E. is an Associate Professor in Aerospace Engineering at Saint Louis University, having worked there since 2010. He received his Bachelor of Science in Aerospace Engineering and Master of Science in Engineering Physics from the University of Virginia in 1990 and 1991, respectively. His Ph.D. in Planetary Science was completed at the Massachusetts Institute of Technology in 1997. He is an Associate Fellow in AIAA, a member of AAS/DPS and AGU, and he has been an author or co-author on more than 75 journal and conference papers. His main research areas are Computational Fluid Dynamics, Flow Control, Plasma Actuators, and Planetary Atmospheres.



Sanjay Jayaram completed Master of Science in Mechanical Engineering in 1998 and Ph. D in 2004 from University of Central Florida, USA. He is currently an Associate Professor in Aerospace Engineering at Saint Louis University, USA. He is an Associate Member of AIAA. He has published more than 30 research papers in reputed international conferences and journals. His main research work focuses on Advanced Control Systems, applications to Autonomous Vehicles and bio-inspired Applied Aerodynamics.

